Functional characterization of protein-tyrosine phosphatases in zebrafish development using image analysis.

Runtuwene, V.J.

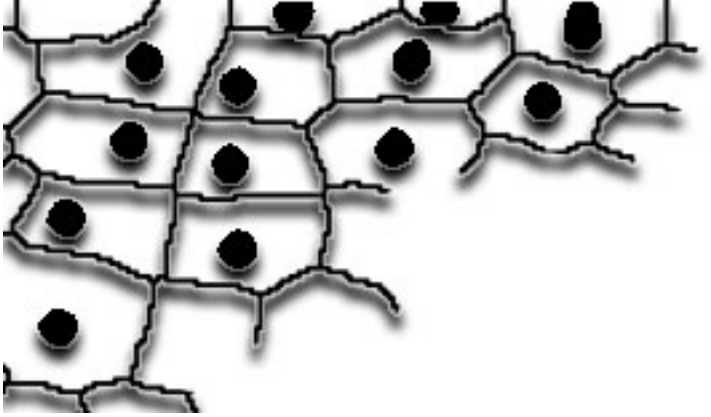

1

Introduction

1 Zebrafish

The zebrafish model system has proven to be invaluable to the study of vertebrate embryogenesis, as human disease models, cancer models and epigenetic research [1-3]. Many features inherent to zebrafish make the system an extraordinarily useful and versatile framework for addressing molecular biological issues. First, zebrafish are relatively easy to maintain, including a comparatively low housing cost [2, 4]. Second, there is a very high fecundity, producing a high number of translucent embryos, which develop rapidly and *ex utero*. As a result, collection of the embryos is straightforward, as is their manipulation. Third, they have a short generation time (3 months), which is evidently advantageous to genetic studies [4]. Additional benefits go hand in hand with the ongoing innovation in parallel fields of research, adding remarkable techniques to the zebrafish genetics toolkit. The advent of morpholino (MO) knockdown technology provided the first method of reverse genetics [5]. This method allowed for direct, albeit transient, interference with the translation of a target gene in embryos by morpholino micro-injection, in contrast to forward genetic techniques, which require multiple rounds of incrossing to perform functional gene studies. TILLING (targeted induced local lesions in genome) provided another reverse genetics method for generating zebrafish knockouts [6, 7] Recently, the use of designed zinc-finger nucleases has proven to be an even more efficient reverse genetics approach [8]. Reverse genetics applications, in their turn, benefit greatly from the assembly of the zebrafish genome [9]. Progressions in the field of transgenesis have developed methods for generating specific zebrafish lines, which have now become standard protocols, available in many laboratories [10, 11]. Further, extraordinary advances in the development of new fluorescent markers (for a review [12]), and groundbreaking steps in imaging technology (for a review [13]), continue to allow for a higher resolution analysis of cellular structure, dynamics, and signaling. In this thesis we utilized the zebrafish system to study the role of protein-tyrosine phosphatases (PTPs) in early development.

2 Gastrulation in zebrafish

Early morphogenesis is very similar in all vertebrates. Variations found between classes of animals are most likely due to differences in the structure of the egg, more exactly the amount of yolk present [14]. As in all vertebrates, fertilization of the zebrafish oocyte, results in a one cell stage zygote. The zygote consists of a large cell on top of a bigger yolk. This stage is followed by the morula stage throughout which six rounds of cell division occur, resulting in a mass of cells on top of the yolk with a combined volume roughly equal to that of the first cell. During the blastula stage, which starts

at the 128-cell stage, cell division continues, the enveloping layer (a single cell layer of larger cells which surrounds the entire embryo) is created and at 4 hours post fertilization the yolk domes into the cells at the animal pole in a process called epiboly. This process, during which the cells radially intercalate, results in a thinnig layer of cells gradually spreading vegetally over the yolk. When the cells have covered 50% of the yolk, internalization of cells at the margin starts and marks the onset of gastrulation [15].

During gastrulation, the embryo is reshaped from an evidently undiversified blastula stage embryo to a multi-layered elongated framework consisting of three germ layers containing clearly defined structures. During this impressive remodeling the cells, and consequently the anlagen, are repositioned according to their future arrangement along the anterio- posterior axis (Fig. 1 A-E) [14]. At 50% epiboly some anlagen, like the precursor cells of forebrain, midbrain and hindbrain, are already positioned in accordance with the later conformation. However, the extent of reorganization is perhaps best exemplified by the change in proximity of the forebrain and the prechordal plate. These organs are, at the start of gastrulation, at opposing poles of the embryo, the former at the animal and the latter at the vegetal pole (Fig. 1 A). Ultimately, adjacent to each other, they will constitute the most anterior structure of the embryo by the end of gastrulation (Fig. 1 D).

The reshaping of the embryo is coordinated by 4 morphogenetic cell movements: internalization, epiboly, convergence and extension (Fig. 1 F-I). Internalization (Fig. 1 F, purple arrow) describes the migration of the mesendodermal precursor cells through the blastoderm margin, which is the position where the enveloping layer makes contact with the yolk syncytial layer (a layer consisting of nuclei situated at the margin, lying directly beneath the blastomeres, within the yolk). The mesendodermal precursors form the hypoblast layer underneath an overlying epiblast (Fig. 1 F). The hypoblast cells at the dorsal side will accumulate, thereby breaking the embryo's radial symmetry, and result in a bulging structure at the dorsal side called the shield, the zebrafish equivalent of the Xenopus Spemann-Mangold organizer (Fig. 1 G) [16-18]. While the epiblast continues epiboly, the hypoblast cells at the shield position migrate anteriorly, moving separately from the overlying layer (Fig. 1 G, dashed turquoise arrow). Epiblast and hypoblast are physically separated by Brachet's cleft. The convergence and extension (CE) movements describe the movement of the lateral cells towards the midline (convergence) and dorsal cell populations in the anterior direction (extension) (Fig. 1 G-I; convergence, blue arrows; extension, turquoise arrows). Medio-lateral cell intercalation at the dorsal side causes the anterior-posterior axis of the embryo to extend. The ventral mesodermal cells however do not converge toward the midline and migrate vegetally, engaging solely in epiboly movements (Fig. 1 G, H; red arrows) [19]. Cell behaviours are variable

depending on the position within the embryo. This difference in behaviour is also reflected in the differences at the cellular level of these populations. During late gastrulation, a large proportion of the mesodermal and ectodermal cells at the dorsal side are more medio-laterally elongated than the ventral mesodermal cells [20-22]. Active medio-lateral polarization, and intercalation of the migrating cells are critical for proper CE movements. Moreover, analysis of cellular morphology of the dorsal ectoderm and mesoderm in CE defected phenotypes often reveal a loss of cell polarization.

3 Genetic regulation of CE movements

In order to choreograph simultaneous cell movements resulting in a net displacement of an entire cell population, the cells are required to collectively polarize in a common direction, as the sum of random singular cell movements would sum up to a zero total displacement. This alignment of the orientations of cells is called planar cell polarity (PCP), and it represents a basic requirement for the establishment of the bilaterally symmetrical body axis during zebrafish gastrulation.

Non-canonical Wnt/PCP pathway

The PCP pathway has been studied to great extent in *Drosophila melanogaster.* Mutations in the components of this pathway have been shown to result in randomization/disorganization in the surface bristles on the thorax, the hairs on the wings, and the photoreceptors in the eye [23-28]. The core components of this pathway identified in Drosophila are *strabismus (stbm)/ van Gogh* (*vang*), *frizzled (fz)*, *disheveled (dsh* or *dvl)*, , *starry night* (*stan*) / *flamingo* (*fmi*), *prickle* (*pk*), and *diego* (*dgo*) [29, 30]. More downstream components are small GTPases RhoA and Rac, and the RhoA effector dRok [31-33]. The mechanism for the establishment of *Drosophila* wing hair cell polarity is a well-studied system utilizing the PCP pathway (Fig. 2A). In wildtype flies every cell produces a single hair, which is aligned along the proximal-distal axis of the wing at the distal membrane of the cell. The PCP pathway controls the number of hairs produced by the cells as well as their subcellular position and the global alignment of the hairs within the wing epithelium. While the mutation of the core components results in defects of the global alignment and subcellular position, the disruption of downstream components results in an increase in the number of hairs produced from a single cell [31-34]. In concordance with a role in cell polarity, several core components of the PCP pathway have a preferential subcellular localization on either the proximal or distal membranes. *Stbm* and *pk* are mostly detected on the proximal membrane and *fz*, *dvl,* and *dgo* on the distal membrane (Fig. 2B). *Fmi* on the other hand is located on both membranes. Other PCP elements like *dachsous* (*ds*) and *four-jointed* (*fj*) have been identified, which show expression gradients

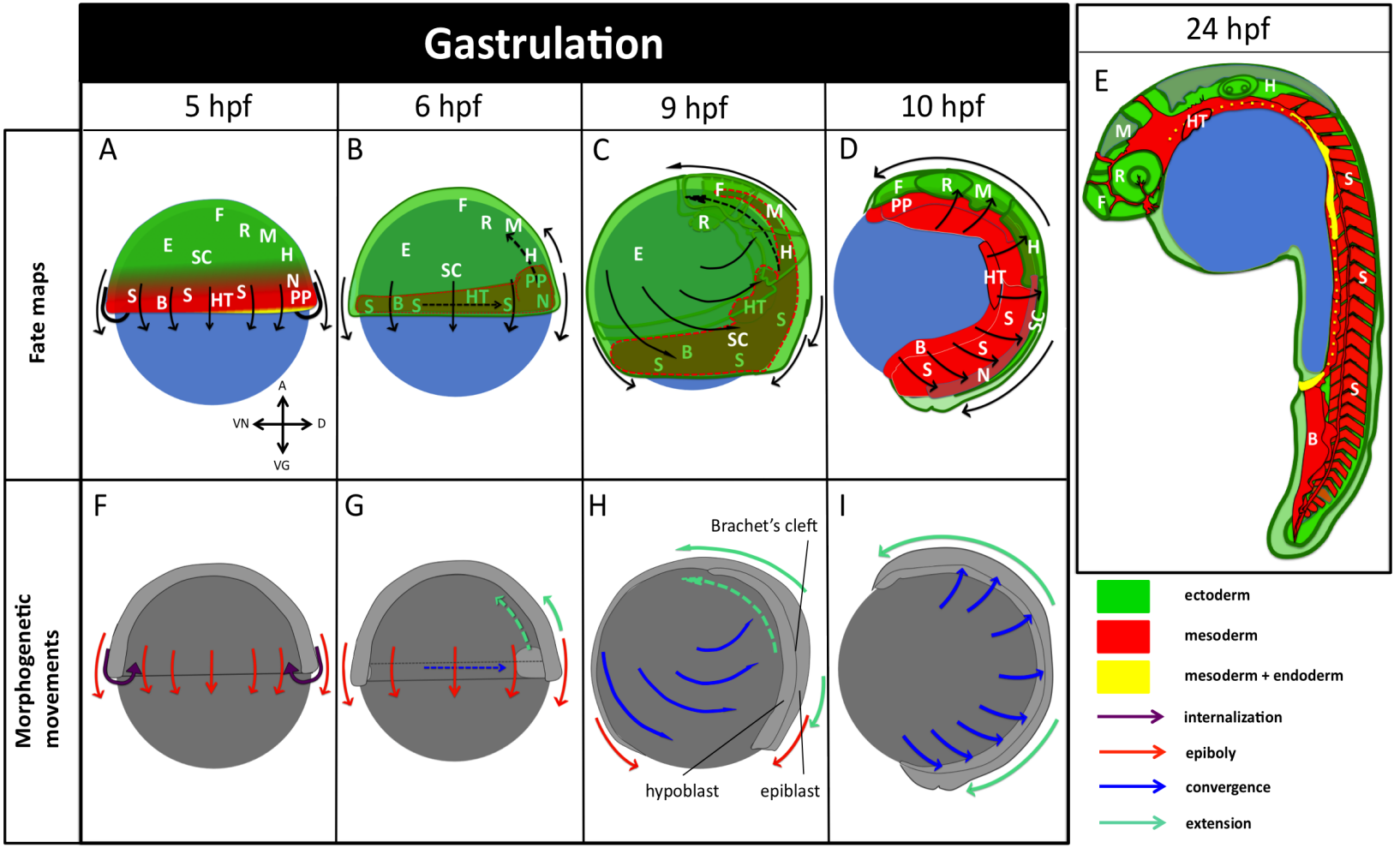
Gastrulation
5 hpf
6 hpf
9 hpf
10 hpf
Fate maps
Morphogenetic movements
A
B
C
D
E
F
G
H
I
24 hpf
F
R
M
E
SC
H
N
S
B
HT
PP
A
VN
D
VG
Brachet's cleft
hypoblast
epiblast
ectoderm
mesoderm
mesoderm + endoderm
internalization
epiboly
convergence
extension

Figure 1: Gastrulation stage fate maps and morphogenetic movements. animal (A), vegetal (VG), dorsal (D), and ventral (VN) directions are indicated in A. The morphogenetic movements are shown using black arrows in A-D. A: Lateral view of a fate map at 50 % epiboly stage (5 hpf). Precursors of the germ layers are arranged along the animal-vegetal axis. The layers are shown with gradient borders since the precursor cells are interspersed at the boundaries rather than showing clear seperation. Several ectodermal and mesodermal anlagen are indicated [105-110]. Yellow indicates both mesodermal and endodermal precursors, modified from [111]. B: Lateral view of a fate map at shield stage (6 hpf), showing the positions of the mesodermal precursors after internalization, inferred from [111]. Cell fates lying within the underlying hypoblast are indicated by a green font. C: Lateral view of a fate map at 90% epiboly (9 hpf). Cell fates lying within the underlying hypoblast are indicated by a green font. Position of the spinal cord is inferred from [112], modified from [111]. D: Lateral view of a fate map at bud stage (10 hpf). Regions shown are approximations derived from the expression of marker genes (ZFIN.org). Modified from [111]. E: Lateral view of a fate map at 24 hpf. The rearrangement of the structures (forebrain, midbrain, hindbrain, heart, retina, somites and vascular system) derived from the anlagen in previous stages is shown (A-D) [15, 107, 110]. Yellow indicates endoderm. F: Cross section of 50 % epiboly stage embryo. Arrows indicate epiboly (red) and internalization (purple) cell movements. G: Cross section of shield stage embryo. Epiboly (red), convergence (blue) and extension (turquoise) movements are indicated. H: Cross section of 90% epiboly stage embryo. Epiboly (red), convergence (blue) and extension (turquoise) movements are indicated. I: Cross section of bud stage embryo. Convergence (blue) and extension (turquoise) movements are indicated. Abbreviations: F, forebrain; R, retina; M, midbrain; H, hindbrain; E, epidermis; SC, spinal cord; N, notochord; PP, prechordal plate; S, somites; B, blood; HT, heart.

along the proximal–distal axis. *Ds* shows a high expression in the distal region, which gradually declines towards the proximal region and the situation has been shown to be inverted for the expression of *fj* (Fig. 2B). A third gradient is formed by the inhibitory activity of *Ds* on *fat* (*ft*), which shows an even expression along the tissue. The interaction results in an activity gradient with the highest activity in the distal region (Fig. 2B) [35, 36]. It has been hypothesized that Ft and Ds form asymmetric heterodimers, which interact with the PCP core components resulting in the observed asymmetric distribution [35, 37]. Another hypothesis suggests that Fj is a Golgi kinase which regulates Ft and Ds by phosphorylation [38].

In vertebrates, homologs of the core components of the *Drosophila* PCP pathway, are required for the generation of the highly organized structure of the auditory and vestibular epithelia. Structurally reminiscent of the *Drosophila* wing epithelium, these epithelia consist of hair cells with clear planar polarization of an asymmetrically located kinocilium and adjacent stereocilia. The hair cells in the semicircular canals of the vestibular labyrinth are unidirectionally oriented along the long axis of each canal. The cochlear hair cells within the auditory system are organized in V-shaped patterns, which point to the periphery of the cochlea (Fig. 2C). The characteristic orientation of the hair cells in these tissues showed a disrupted phenotype in mice harboring core PCP component mutations [25,

39-43]. The parallels of these tissues with the *Drosophila* wing epithelium are even clear at the subcellular level, where components of the mammalian systems mimic the *Drosophila* subcellular organization to a very high degree: Pk and Vangl on the medial side and Fz, Dvl and Dgo on the lateral (Fig. 2D). Due to duplication events in vertebrates, not all single mutations in core PCP components result in a PCP- related phenotype [44]. The existence of redundant gene duplicates of several PCP core components like *fz3* and *fz6 [41], and dvl1* and *dvl2* [45] make it necessary to interfere with the expression of both genes to generate a PCP-related phenotype.

Non-canonical Wnt signaling, which shares many components with the PCP pathway, is activated by Wnt5 and Wnt11 and is distinguished from canonical Wnt signaling in the fact that it transduces its signals independent from β–catenin [46, 47]. Upon binding of Wnt5 or Wnt11 to Fz, Dsh is recruited to the plasma membrane where it interacts with Daam1 [48, 49]. This activation of Daam1 results, through interaction with RhoGEFs like WGEF, in the activation of the small GTPase RhoA, which propagates the signal to Rok2 [50-52]. Non-canonical Wnt signaling, through direct interaction with the Fz-Dsh complex, also activates the small GTPase Rac1, which transduces the signal to C-Jun N-terminal kinase (JNK) (Fig. 3) [53, 54]. This signaling ultimately results in the remodeling of the cell cytoskeleton and, as a consequence, the establishment of polarization. Non-canonical Wnt signaling regulates CE movements by establishing the necessary polarization of the ectodermal and mesodermal cells during gastrulation [19]. Mutants, which harbor mutations in components of the non-canonical Wnt pathway, display defects in CE movements, and a loss of cell polarization in dorsal neurectoderm, and paraxial and axial mesoderm (Fig. 2E) [19, 22, 55-57]. Very similar to the situation in PCP signaling, several components are subcellularly localized in the migrating cells, with Fz and Dsh at the distal membrane and Pk and Vangl at the proximal membrane [58-60]. While the subcellular localization of these components is reminiscent of PCP signaling as it is found in epithelial tissues, it remains to be shown whether these elements perform a functionally similar role within these embryonic tissues.

Other pathways

Stat3 signaling has been implied to regulate CE movements. It has been suggested that Stat3 non-autonomously activates non-canonical Wnt signaling in neighbouring cells by enabling the expression of an as of yet unknown downstream target in the shield region, which forms an extracellular gradient. This gradient is required for lateral mesendodermal cells to sense the direction of convergence movements via the activation of RhoA downstream of Dsh [61].

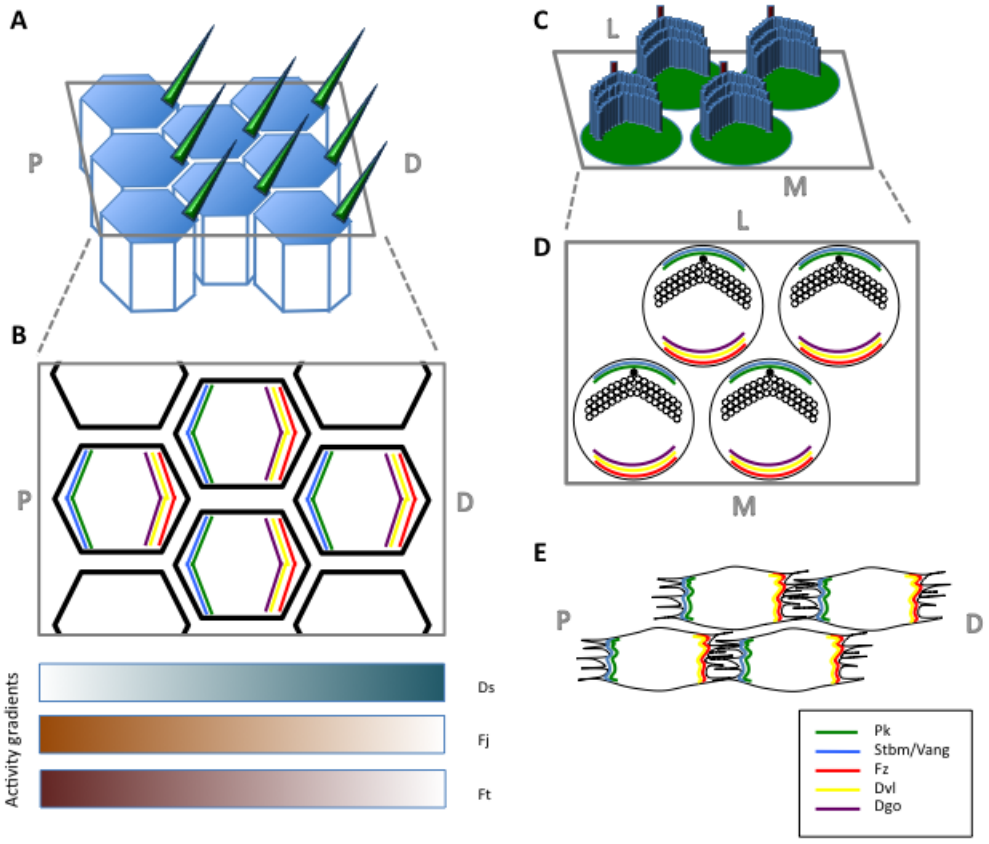

Figure 2. Planar cell polarity pathway. A: Schematic representation of Drosophila wing epithelial cells producing one hair each (presented in green). Proximal (P) and distal (D) directions are indicated. B: Schematic representation showing the subcellular distribution of PCP proteins Prickle (Pk), Strabismus (Stbm), Frizzled (Fz), Dishevelled (Dvl), and Diego (Dgo) and activity gradients over the wing epithelium of Dachsous (Ds), Four-jointed (Fj), and Fat (Ft). Proximal (P) and distal (D) directions are indicated. C: Schematic representation of cochlea hair cells with a big kinocilium (indiciated in red), and stereocilia (indicated in blue) organized in a V-shape. Lateral (L) and medial (M) directions are indicated. D: Schematic representation of intracellular distribution of PCP components Pk, Stbm, Fz, Dvl, and Dgo in cochlea hair cells . E: Schematic representation of the distribution of PCP components Pk, Stbm, Fz, and Dvl in polarized mesodermal migrating cells in CE movements. Proximal (P) and distal (D) directions are indicated.

Bmp signaling has also been proposed to contribute to CE movements. It is expressed as a gradient, which is high at the ventral side and low at the dorsal. As Bmp signaling negatively regulates Ca^{2+}/cadherin-dependent cell-cell adhesiveness, the gastrula is subdivided in different migratory regions. The resulting lower cell–cell adhesion at the ventral side and higher adhesiveness at the dorsal side contributes to cell migration towards the dorsal side [62].

Csk, Fyn and Yes have been shown to activate RhoA in parallel to non-

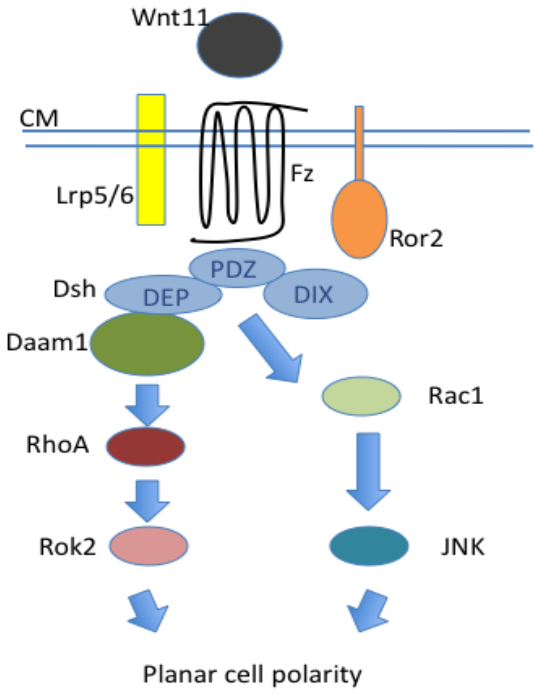

Figure 3. Non-canonical Wnt signaling pathway. Dishevelled (Dsh/Dvl) is recruited by Frizzled upon Wnt11 (ligand) binding. The Wnt-Frizzled complex interacts with Ror2 and Lrp5/6. Rac1 is activated through Dsh and RhoA through Daam1, which binds the DEP domain of Dishevelled. RhoA activates Rok2 and Rac1 activates JNK, both leading to planar cell polarity signaling.

canonical Wnt signaling [63, 64]. Other factors which have been implicated to have a role in CE are ephrins [65], Slit/Robo [66], Scribble-1 [67], Widerborst [68], Cyclooxygenase [69], and Has2 [70].

4 Ptps in zebrafish development

Reversible tyrosine phosphorylation of proteins is a key mechanism for transducing inter- and intracellular stimuli, and acts as a highly dynamic molecular switch between different activation states of signaling molecules, and consequently plays an important role in cellular processes like migration, proliferation, and differentiation [71-74]. Given its elemental role, it is not surprising that disruption of the synergy between protein-tyrosine kinases (PTKs) and phosphatases (PTPs) underlies many human diseases and developmental defects [75-80]. While great advances have been made in the field of research of PTKs, our understanding of the function of PTPs is lagging behind. This discrepancy is largely attributable to the wrongful assumption that PTPs are mere household enzymes with low substrate specificities, which plainly counter the effects of the PTKs by continuous dephosphorylation [75]. By now, many studies have acknowledged PTPs to be a very diverse family of proteins with highly specific roles in both development and disease [81]. For example, following the demonstration of direct interaction between the insulin receptor and PTP1B [82], the first PTP purified and sequenced [83], PTP1B knockout mice were shown to have enhanced insulin sensitivity, specifically in liver and muscle tissues [84]. Furthermore, the PTP1B locus maps to

a chromosomal region, 20q13.1-q13.2 [85], identified as a quantitative trait locus linked to diabetes and obesity [86]. PTPRO, a type III transmembrane PTP, plays an essential role in the development and function of the sensory nervous system [87]. This PTP is expressed in mouse dorsal root ganglion neurons. Ablation results in both a significant decrease in the number of peptidergic nociceptive neurons, and concomitant aberrations in their spinal pathfinding. Adult PTPRO knockout mice showed defects in nociception and sensorimotor coordination [87]. Mouse knockout models have contributed greatly to the elucidation of PTP functions. However, their *in utero* development constitutes an obvious complication when investigating events during early embryogenesis.

Given the many advantages of using zebrafish for studies of early vertebrate development, enumerated earlier, we used the zebrafish model to elucidate functions of PTPs in CE cell movements during gastrulation. Previously, we have identified all members of the family of classical PTPs in the zebrafish genome by blasting human PTP domains against the zebrafish Ensembl genome sequence (Zv8). With the exception of three PTP genes, homologs of the entire family of classical PTPs has been identified (Fig. 4). Fourteen genes have been found to have undergone duplication, which is not uncommon in zebrafish [88]. These duplicates have been hypothesized to result from a genome duplication event during teleost evolution [89]. Comparative sequence analysis of the human and zebrafish PTPs demonstrated that both protein families are closely related and highly comparable. Furthermore, detailed analysis of the spatio-temporal expression patterns of the 48 PTPs during early embryonic development revealed that most zebrafish PTPs are maternally contributed and are broadly expressed during early development, supporting the view of a potential role for PTPs during these stages [88]. A study using very potent generic PTP inhibitors, like peroxivanadate, already indicated that many aspects of egg activation require PTP activity [90]. Here we will review earlier work, which demonstrated that specific zebrafish PTPs are indeed essential for normal development.

The first zebrafish PTP to be cloned was PTP1B. Functional analysis *in vivo* using ectopic expression of wild type and dominant negative PTP1B C213S mutant, demonstrated that expression of wild type PTP1B, but not the catalytically inactive form, resulted in defects in somite formation [91].

It is unclear wether Pez, a FERM domain containing cytosolic PTP, encoded by *Ptpn14* in the zebrafish genome, contains a PTP domain [88]. This protein is transiently expressed at multiple sites, in developing brain, heart, pharyngeal arches, and somites during development. Knockdown by injection of ATG MOs, produces defects in these organsystems. Additionally, overexpression of Pez in epithelial MDCK cells causes epithelial–mesenchymal transition (EMT). Ectopic expression of Pez induces TGFβ signaling in MDCK cells, and, in zebrafish

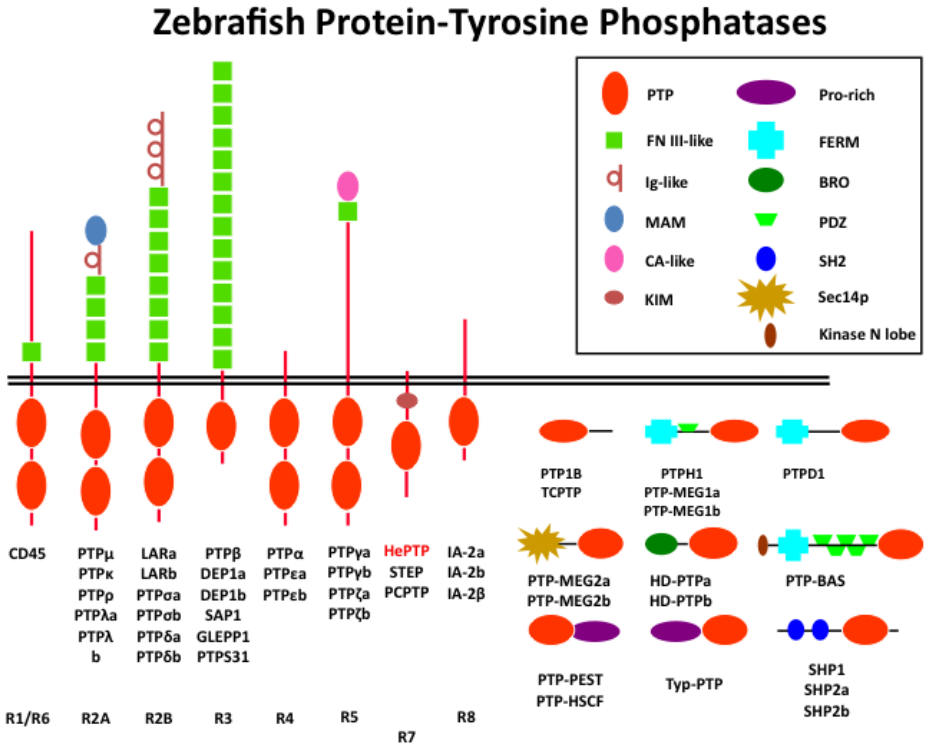

Figure 4. Zebrafish protein tyrosine phosphatases. Schematic representation of PTPs as they are found in the zebrafish genome. Human orthologs not identified in the zebrafish genome are indicated in red. Duplicated gene names were appended with "a" or "b".

embryos, TGFβ3, which is coexpressed with Pez, is lost upon knockdown of Pez. These results indicate a critical role for Pez in organogenesis by induction of TGFβ signaling and EMT [92].

Knockdown of *ptpra*, which is maternally contributed and broadly expressed during early development [93], using ATG MOs resulted in specific defects in eye development, which were visible at 3 days post fertilization (dpf). The eyes were smaller and the layered structure of the retina were absent. Interestingly, at 5 dpf concomitant with the loss of knockdown efficiency of the MOs, the lamination of the retina was restored, although significant gaps in the amacrin layer were still observed [94]. In Chapter 2, we demonstrate that *ptpra* -/- mutants and morphants display, next to eye defects, CE defects.

Ptprua, which encodes the protein PTPψ and has an ohnolog *ptprub* [88] is shown to be critical for the normal functioning of the somitogenesis clock. Injection of ATG MOs in one cell stage embryos resulted in a disruption of the segmental pattern of the embryo. Analysis of the cyclic genes in *ptprua* morphant embryos indicates regulation of the somitogenesis clock upstream or in parallel

with Delta/Notch signaling. Moreover, *in situ* analysis of several markers revealed that *ptprua* morphants display CE defects [95]. In chapter 6, by confocal imaging of the presomitic mesoderm during gastrulation and subsequent polarization analysis, we provide direct evidence of the loss of cell polarization during CE movements in *ptprua* morphants.

Zebrafish Shp2a, encoded by the gene *ptpn11a*, is broadly expressed in early development [96]. A potential ohnolog, *ptpn11b*, has been identified [88], however its expression and function are still undetermined. MO mediated Shp2a knockdown causes CE defects, demonstrated by *in situ* analysis of well-established markers for CE and cell tracking experiments using caged fluorescein dextran. Successful rescue experiments wherein Shp2 MOs were coinjected with mRNA of constitutively active variants of the Src family kinases Fyn and Yes, and the small GTPase RhoA, provided evidence that Shp2a signals upstream of these signaling molecules [96], in concordance with the mouse knockout model. Shp2 null mice die at mid-gestation, displaying defects in the node, notochord and posterior elongation, indicating severe gastrulation defects [97]. Shp2 mutations underlie human Noonan and LEOPARD syndrome [98, 99]. These two conditions have a set of overlapping symptoms, including short stature, craniofacial abnormalities, and cardiac defects. Intriguingly, embryos injected with Shp2a mRNA harboring Noonan or LEOPARD mutations display CE defects during gastrulation and at later stages, defects reminiscent of the symptoms of human patients [96]. These results indicate that zebrafish can be used to model human diseases.

5 Image processing approaches for autosegmentation

Remarkable advances are being made in the field of biomedical imaging. New lightsheet technology is pushing the envelope regarding speed, sensitivity, spectral and depth resolution [100]. This is being complemented by the development of a veritable rainbow of brighter and more sensitive fluorescent probes. Nowadays, most standard laboratories have access to confocal and multi-photon microscopes, able to generate 3-D and 4-D (timelapse) data sets. A vast amount of morphological information at cellular resolution can be extracted from these huge data sets. This situation echoes a similar problem, which posed itself with the enhancements in sequencing technology in the post-genomic era. The massive availability of genomic information, found in online databases, warranted the development of data mining, which was facilitated by the advent of fast and accurate search algorithms. While complex formulas and sophisticated hardware and software have been developed for detecting cellular features in images [100-104], these technologies are usually not available in standard biological/ biomedical laboratories.

Critical parameters in determining CE defects on a cellular level

are migration patterns and cell shape/polarization [19]. However, since the gastrulation cell movements involve the migration of entire layers of cells, individual cell readings are less relevant than the determination of the net movement of a group of cells. For a similar reason, a relatively high number of cells needs to be analyzed for polarization, to be able to determine whether a randomization of polarization has occurred. Manual collection of these types of data from confocal data sets is tedious, time-consuming, error-prone, and subjective.

6 *Outline of this thesis*

In this thesis we use the zebrafish system to identify members of the PTP family, having a role in CE movements during gastrulation. The aim is not only to identify, characterize the function and interactions of these genes, but also to generate fast and reliable methods to quantify morphological parameters of CE movements like tissue migration and polarization.

Tail length is a simple but effective morphological measurement used to identify CE phenotypes. While it is not a conclusive parameter to identify CE defects, we argue that it can be used to identify proteins involved in the same biochemical pathway by combining partial gene knockdown. Applying varying MO concentrations, this method is used to identify molecules regulating RhoA activity independent of non-canonical Wnt signaling in Chapter 2 and 3. In these chapters we also introduce an algorithm for automated detection of cell migration and a new method for more efficient detection of cell polarization.

In chapter 4, we identify a novel Noonan-associated gain-of-function *NRAS* mutation. Using mRNA- injections, we go on to show that this mutation and other Noonan-associated mutations can also be used to model Noonan syndrome in zebrafish. Moreover, we demonstrate the relative ease-of-use (addition to the water) of chemical compounds in zebrafish to modify aberrant RAS-MAPK signaling.

In chapter 5, we introduce an automated algorithm for detection of mesodermal cell membranes, and a novel method for presenting polarization data, providing a more straightforward representation of orientation and elongation of cells within a layer.

In chapter 6, we perform a screen of the entire PTP family. Candidate genes are analyzed in detail for convergence and extension defects, by tail length measurements, *in situ* hybridization and confocal microscopy-based cell shape analysis, yielding one *bona fide* novel PTP with a role in convergence and extension cell movements. We also provide direct proof of the cell polarization defects underlying the CE defects in *ptpn11a* and *ptprua* morphants.

References

1. Lieschke, G.J. and P.D. Currie, Animal models of human disease: zebrafish swim into view. Nat Rev Genet, 2007. 8(5): p. 353-67.
2. Ali, S., et al., Zebrafish embryos and larvae: a new generation of disease models and drug screens. Birth Defects Res C Embryo Today, 2011. 93(2): p. 115-33.
3. Mudbhary, R. and K.C. Sadler, Epigenetics, development, and cancer: zebrafish make their ARK. Birth Defects Res C Embryo Today, 2011. 93(2): p. 194-203.
4. Wixon, J., Featured organism: Danio rerio, the zebrafish. Yeast, 2000. 17(3): p. 225-31.
5. Nasevicius, A. and S.C. Ekker, Effective targeted gene 'knockdown' in zebrafish. Nat Genet, 2000. 26(2): p. 216-20.
6. Wienholds, E., et al., Target-selected inactivation of the zebrafish rag1 gene. Science, 2002. 297(5578): p. 99-102.
7. Wienholds, E., et al., Efficient target-selected mutagenesis in zebrafish. Genome Res, 2003. 13(12): p. 2700-7.
8. Doyon, Y., et al., Heritable targeted gene disruption in zebrafish using designed zinc-finger nucleases. Nat Biotechnol, 2008. 26(6): p. 702-8.
9. Flicek, P., et al., Ensembl 2011. Nucleic Acids Res, 2011. 39(Database issue): p. D800-6.
10. Grabher, C. and J. Wittbrodt, Recent advances in meganuclease-and transposon-mediated transgenesis of medaka and zebrafish. Methods Mol Biol, 2008. 461: p. 521-39.
11. Udvadia, A.J. and E. Linney, Windows into development: historic, current, and future perspectives on transgenic zebrafish. Dev Biol, 2003. 256(1): p. 1-17.
12. Tsien, R.Y., Nobel lecture: constructing and exploiting the fluorescent protein paintbox. Integr Biol (Camb), 2010. 2(2-3): p. 77-93.
13. Megason, S.G. and S.E. Fraser, Imaging in systems biology. Cell, 2007. 130(5): p. 784-95.
14. Schoenwolf, G.C. and J.L. Smith, Gastrulation and early mesodermal patterning in vertebrates. Methods Mol Biol, 2000. 135: p. 113-25.
15. Kimmel, C.B., et al., Stages of embryonic development of the zebrafish. Dev Dyn, 1995. 203(3): p. 253-310.
16. Warga, R.M. and C.B. Kimmel, Cell movements during epiboly and gastrulation in zebrafish. Development, 1990. 108(4): p. 569-80.
17. Montero, J.A., et al., Shield formation at the onset of zebrafish gastrulation. Development, 2005. 132(6): p. 1187-98.

18. Montero, J.A. and C.P. Heisenberg, Gastrulation dynamics: cells move into focus. Trends Cell Biol, 2004. 14(11): p. 620-7.
19. Myers, D.C., D.S. Sepich, and L. Solnica-Krezel, Convergence and extension in vertebrate gastrulae: cell movements according to or in search of identity? Trends Genet, 2002. 18(9): p. 447-55.
20. Concha, M.L. and R.J. Adams, Oriented cell divisions and cellular morphogenesis in the zebrafish gastrula and neurula: a time-lapse analysis. Development, 1998. 125(6): p. 983-94.
21. Myers, D.C., D.S. Sepich, and L. Solnica-Krezel, Bmp activity gradient regulates convergent extension during zebrafish gastrulation. Dev Biol, 2002. 243(1): p. 81-98.
22. Topczewski, J., et al., The zebrafish glypican knypek controls cell polarity during gastrulation movements of convergent extension. Dev Cell, 2001. 1(2): p. 251-64.
23. Shimada, Y., et al., Asymmetric colocalization of Flamingo, a seven-pass transmembrane cadherin, and Dishevelled in planar cell polarization. Curr Biol, 2001. 11(11): p. 859-63.
24. Veeman, M.T., J.D. Axelrod, and R.T. Moon, A second canon. Functions and mechanisms of beta-catenin-independent Wnt signaling. Dev Cell, 2003. 5(3): p. 367-77.
25. McNeill, H., Planar cell polarity: keeping hairs straight is not so simple. Cold Spring Harb Perspect Biol, 2010. 2(2): p. a003376.
26. Gubb, D. and A. Garcia-Bellido, A genetic analysis of the determination of cuticular polarity during development in Drosophila melanogaster. J Embryol Exp Morphol, 1982. 68: p. 37-57.
27. Chae, J., et al., The Drosophila tissue polarity gene starry night encodes a member of the protocadherin family. Development, 1999. 126(23): p. 5421-9.
28. Taylor, J., et al., Van Gogh: a new Drosophila tissue polarity gene. Genetics, 1998. 150(1): p. 199-210.
29. Fanto, M. and H. McNeill, Planar polarity from flies to vertebrates. J Cell Sci, 2004. 117(Pt 4): p. 527-33.
30. Feiguin, F., et al., The ankyrin repeat protein Diego mediates Frizzled-dependent planar polarization. Dev Cell, 2001. 1(1): p. 93-101.
31. Eaton, S., R. Wepf, and K. Simons, Roles for Rac1 and Cdc42 in planar polarization and hair outgrowth in the wing of Drosophila. J Cell Biol, 1996. 135(5): p. 1277-89.
32. Strutt, D.I., U. Weber, and M. Mlodzik, The role of RhoA in tissue polarity and Frizzled signalling. Nature, 1997. 387(6630): p. 292-5.
33. Winter, C.G., et al., Drosophila Rho-associated kinase (Drok) links Frizzled-mediated planar cell polarity signaling to the actin cytoskeleton. Cell, 2001. 105(1): p. 81-91.

34. Wong, L.L. and P.N. Adler, Tissue polarity genes of Drosophila regulate the subcellular location for prehair initiation in pupal wing cells. J Cell Biol, 1993. 123(1): p. 209-21.
35. Ma, D., et al., Fidelity in planar cell polarity signalling. Nature, 2003. 421(6922): p. 543-7.
36. Yang, C.H., M.A. Simon, and H. McNeill, mirror controls planar polarity and equator formation through repression of fringe expression and through control of cell affinities. Development, 1999. 126(24): p. 5857-66.
37. Yang, C.H., J.D. Axelrod, and M.A. Simon, Regulation of Frizzled by fat-like cadherins during planar polarity signaling in the Drosophila compound eye. Cell, 2002. 108(5): p. 675-88.
38. Ishikawa, H.O., et al., Four-jointed is a Golgi kinase that phosphorylates a subset of cadherin domains. Science, 2008. 321(5887): p. 401-4.
39. Vladar, E.K., D. Antic, and J.D. Axelrod, Planar cell polarity signaling: the developing cell's compass. Cold Spring Harb Perspect Biol, 2009. 1(3): p. a002964.
40. Kelly, M. and P. Chen, Shaping the mammalian auditory sensory organ by the planar cell polarity pathway. Int J Dev Biol, 2007. 51(6-7): p. 535-47.
41. Wang, Y., N. Guo, and J. Nathans, The role of Frizzled3 and Frizzled6 in neural tube closure and in the planar polarity of inner-ear sensory hair cells. J Neurosci, 2006. 26(8): p. 2147-56.
42. Wang, J., et al., Dishevelled genes mediate a conserved mammalian PCP pathway to regulate convergent extension during neurulation. Development, 2006. 133(9): p. 1767-78.
43. Etheridge, S.L., et al., Murine dishevelled 3 functions in redundant pathways with dishevelled 1 and 2 in normal cardiac outflow tract, cochlea, and neural tube development. PLoS Genet, 2008. 4(11): p. e1000259.
44. Wansleeben, C. and F. Meijlink, The planar cell polarity pathway in vertebrate development. Dev Dyn, 2011. 240(3): p. 616-26.
45. Wang, J., et al., Regulation of polarized extension and planar cell polarity in the cochlea by the vertebrate PCP pathway. Nat Genet, 2005. 37(9): p. 980-5.
46. Boutros, M., et al., Dishevelled activates JNK and discriminates between JNK pathways in planar polarity and wingless signaling. Cell, 1998. 94(1): p. 109-18.
47. Moon, R.T., et al., Xwnt-5A: a maternal Wnt that affects morphogenetic movements after overexpression in embryos of Xenopus laevis. Development, 1993. 119(1): p. 97-111.
48. Wong, H.C., et al., Direct binding of the PDZ domain of Dishevelled to a conserved internal sequence in the C-terminal region of Frizzled. Mol Cell, 2003. 12(5): p. 1251-60.
49. Punchihewa, C., et al., Sequence requirement and subtype specificity

in the high-affinity interaction between human frizzled and dishevelled proteins. Protein Sci, 2009. 18(5): p. 994-1002.
50. Alberts, A.S., Diaphanous-related Formin homology proteins. Curr Biol, 2002. 12(23): p. R796.
51. Higgs, H.N., Formin proteins: a domain-based approach. Trends Biochem Sci, 2005. 30(6): p. 342-53.
52. Liu, W., et al., Mechanism of activation of the Formin protein Daam1. Proc Natl Acad Sci U S A, 2008. 105(1): p. 210-5.
53. Rosso, S.B., et al., Wnt signaling through Dishevelled, Rac and JNK regulates dendritic development. Nat Neurosci, 2005. 8(1): p. 34-42.
54. Habas, R., I.B. Dawid, and X. He, Coactivation of Rac and Rho by Wnt/Frizzled signaling is required for vertebrate gastrulation. Genes Dev, 2003. 17(2): p. 295-309.
55. Wallingford, J.B., S.E. Fraser, and R.M. Harland, Convergent extension: the molecular control of polarized cell movement during embryonic development. Dev Cell, 2002. 2(6): p. 695-706.
56. Jessen, J.R., et al., Zebrafish trilobite identifies new roles for Strabismus in gastrulation and neuronal movements. Nat Cell Biol, 2002. 4(8): p. 610-5.
57. Wallingford, J.B., et al., Dishevelled controls cell polarity during Xenopus gastrulation. Nature, 2000. 405(6782): p. 81-5.
58. Adler, P.N., Planar signaling and morphogenesis in Drosophila. Dev Cell, 2002. 2(5): p. 525-35.
59. Tree, D.R., et al., Prickle mediates feedback amplification to generate asymmetric planar cell polarity signaling. Cell, 2002. 109(3): p. 371-81.
60. Jenny, A., et al., Prickle and Strabismus form a functional complex to generate a correct axis during planar cell polarity signaling. EMBO J, 2003. 22(17): p. 4409-20.
61. Miyagi, C., et al., STAT3 noncell-autonomously controls planar cell polarity during zebrafish convergence and extension. J Cell Biol, 2004. 166(7): p. 975-81.
62. von der Hardt, S., et al., The Bmp gradient of the zebrafish gastrula guides migrating lateral cells by regulating cell-cell adhesion. Curr Biol, 2007. 17(6): p. 475-87.
63. Jopling, C. and J. Hertog, Essential role for Csk upstream of Fyn and Yes in zebrafish gastrulation. Mech Dev, 2007. 124(2): p. 129-36.
64. Jopling, C. and J. den Hertog, Fyn/Yes and non-canonical Wnt signalling converge on RhoA in vertebrate gastrulation cell movements. EMBO Rep, 2005. 6(5): p. 426-31.
65. Oates, A.C., et al., An early developmental role for eph-ephrin interaction during vertebrate gastrulation. Mech Dev, 1999. 83(1-2): p. 77-94.
66. Yeo, S.Y., et al., Overexpression of a slit homologue impairs convergent

extension of the mesoderm and causes cyclopia in embryonic zebrafish. Dev Biol, 2001. 230(1): p. 1-17.
67. Wada, H., et al., Dual roles of zygotic and maternal Scribble1 in neural migration and convergent extension movements in zebrafish embryos. Development, 2005. 132(10): p. 2273-85.
68. Hannus, M., et al., Planar cell polarization requires Widerborst, a B' regulatory subunit of protein phosphatase 2A. Development, 2002. 129(14): p. 3493-503.
69. Cha, Y.I., et al., Cyclooxygenase-1 signaling is required for vascular tube formation during development. Dev Biol, 2005. 282(1): p. 274-83.
70. Bakkers, J., et al., Has2 is required upstream of Rac1 to govern dorsal migration of lateral cells during zebrafish gastrulation. Development, 2004. 131(3): p. 525-37.
71. Hunter, T., Protein kinases and phosphatases: the yin and yang of protein phosphorylation and signaling. Cell, 1995. 80(2): p. 225-36.
72. van der Geer, P., T. Hunter, and R.A. Lindberg, Receptor protein-tyrosine kinases and their signal transduction pathways. Annu Rev Cell Biol, 1994. 10: p. 251-337.
73. Van Vactor, D., A.M. O'Reilly, and B.G. Neel, Genetic analysis of protein tyrosine phosphatases. Curr Opin Genet Dev, 1998. 8(1): p. 112-26.
74. Clark, E.A. and J.S. Brugge, Integrins and signal transduction pathways: the road taken. Science, 1995. 268(5208): p. 233-9.
75. den Hertog, J., Protein-tyrosine phosphatases in development. Mech Dev, 1999. 85(1-2): p. 3-14.
76. Alonso, A., et al., Protein tyrosine phosphatases in the human genome. Cell, 2004. 117(6): p. 699-711.
77. Hendriks, W.J., et al., Protein tyrosine phosphatases: functional inferences from mouse models and human diseases. FEBS J, 2008. 275(5): p. 816-30.
78. LaForgia, S., et al., Receptor protein-tyrosine phosphatase gamma is a candidate tumor suppressor gene at human chromosome region 3p21. Proc Natl Acad Sci U S A, 1991. 88(11): p. 5036-40.
79. Tartaglia, M., et al., Mutations in PTPN11, encoding the protein tyrosine phosphatase SHP-2, cause Noonan syndrome. Nat Genet, 2001. 29(4): p. 465-8.
80. Wang, Z., et al., Mutational analysis of the tyrosine phosphatome in colorectal cancers. Science, 2004. 304(5674): p. 1164-6.
81. Tonks, N.K., Protein tyrosine phosphatases: from genes, to function, to disease. Nat Rev Mol Cell Biol, 2006. 7(11): p. 833-46.
82. Seely, B.L., et al., Protein tyrosine phosphatase 1B interacts with the activated insulin receptor. Diabetes, 1996. 45(10): p. 1379-85.
83. Tonks, N.K., C.D. Diltz, and E.H. Fischer, Purification of the major pro-

tein-tyrosine-phosphatases of human placenta. J Biol Chem, 1988. 263(14): p. 6722-30.
84. Elchebly, M., et al., Increased insulin sensitivity and obesity resistance in mice lacking the protein tyrosine phosphatase-1B gene. Science, 1999. 283(5407): p. 1544-8.
85. Brown-Shimer, S., et al., Molecular cloning and chromosome mapping of the human gene encoding protein phosphotyrosyl phosphatase 1B. Proc Natl Acad Sci U S A, 1990. 87(13): p. 5148-52.
86. Lembertas, A.V., et al., Identification of an obesity quantitative trait locus on mouse chromosome 2 and evidence of linkage to body fat and insulin on the human homologous region 20q. J Clin Invest, 1997. 100(5): p. 1240-7.
87. Gonzalez-Brito, M.R. and J.L. Bixby, Protein tyrosine phosphatase receptor type O regulates development and function of the sensory nervous system. Mol Cell Neurosci, 2009. 42(4): p. 458-65.
88. van Eekelen, M., et al., Identification and expression of the family of classical protein-tyrosine phosphatases in zebrafish. PLoS One, 2010. 5(9): p. e12573.
89. Postlethwait, J.H., The zebrafish genome in context: ohnologs gone missing. J Exp Zool B Mol Dev Evol, 2007. 308(5): p. 563-77.
90. Wu, W. and W.H. Kinsey, Role of PTPase(s) in regulating Fyn kinase at fertilization of the zebrafish egg. Dev Biol, 2002. 247(2): p. 286-94.
91. van der Sar, A.M., et al., Pleiotropic effects of zebrafish protein-tyrosine phosphatase-1B on early embryonic development. Int J Dev Biol, 1999. 43(8): p. 785-94.
92. Wyatt, L., et al., The protein tyrosine phosphatase Pez regulates TGF-beta, epithelial-mesenchymal transition, and organ development. J Cell Biol, 2007. 178(7): p. 1223-35.
93. van der Sar, A., et al., Expression of receptor protein-tyrosine phosphatase alpha, sigma and LAR during development of the zebrafish embryo. Mech Dev, 2001. 109(2): p. 423-6.
94. van der Sar, A.M., D. Zivkovic, and J. den Hertog, Eye defects in receptor protein-tyrosine phosphatase alpha knock-down zebrafish. Dev Dyn, 2002. 223(2): p. 292-7.
95. Aerne, B. and D. Ish-Horowicz, Receptor tyrosine phosphatase psi is required for Delta/Notch signalling and cyclic gene expression in the presomitic mesoderm. Development, 2004. 131(14): p. 3391-9.
96. Jopling, C., D. van Geemen, and J. den Hertog, Shp2 knockdown and Noonan/LEOPARD mutant Shp2-induced gastrulation defects. PLoS Genet, 2007. 3(12): p. e225.
97. Saxton, T.M., et al., Abnormal mesoderm patterning in mouse embryos mutant for the SH2 tyrosine phosphatase Shp-2. EMBO J, 1997. 16(9): p.

2352-64.
98. Allanson, J.E., Noonan syndrome. J Med Genet, 1987. 24(1): p. 9-13.
99. Gorlin, R.J., R.C. Anderson, and J.H. Moller, The leopard (multiple lentigines) syndrome revisited. Laryngoscope, 1971. 81(10): p. 1674-81.
100. Keller, P.J., et al., Reconstruction of zebrafish early embryonic development by scanned light sheet microscopy. Science, 2008. 322(5904): p. 1065-9.
101. Megason, S.G., In toto imaging of embryogenesis with confocal time-lapse microscopy. Methods Mol Biol, 2009. 546: p. 317-32.
102. Mosaliganti, K., et al., Anisotropic Plate Diffusion Filtering for Detection of Cell Membranes in 3d Microscopy Images. Proc IEEE Int Symp Biomed Imaging, 2010: p. 588-591.
103. Jurrus, E., et al., Detection of neuron membranes in electron microscopy images using a serial neural network architecture. Med Image Anal, 2010. 14(6): p. 770-83.
104. M.A.Luengo-Oroz, L.D., C.Castrcfi, T.SavyK E.Faure, B.Lombardo, and N.P.a.A.S. P.Bourgine, Can voronoi diagram model cell geometries in early sea urchin embryogenesis? ISBI, 2008: p. 504-507.
105. Dougan, S.T., et al., The role of the zebrafish nodal-related genes squint and cyclops in patterning of mesendoderm. Development, 2003. 130(9): p. 1837-51.
106. Gritsman, K., W.S. Talbot, and A.F. Schier, Nodal signaling patterns the organizer. Development, 2000. 127(5): p. 921-32.
107. Keegan, B.R., D. Meyer, and D. Yelon, Organization of cardiac chamber progenitors in the zebrafish blastula. Development, 2004. 131(13): p. 3081-91.
108. Kimmel, C.B., R.M. Warga, and T.F. Schilling, Origin and organization of the zebrafish fate map. Development, 1990. 108(4): p. 581-94.
109. Woo, K. and S.E. Fraser, Specification of the hindbrain fate in the zebrafish. Dev Biol, 1998. 197(2): p. 283-96.
110. Woo, K. and S.E. Fraser, Order and coherence in the fate map of the zebrafish nervous system. Development, 1995. 121(8): p. 2595-609.
111. Schier, A.F. and W.S. Talbot, Molecular genetics of axis formation in zebrafish. Annu Rev Genet, 2005. 39: p. 561-613.
112. Kudoh, T., S.W. Wilson, and I.B. Dawid, Distinct roles for Fgf, Wnt and retinoic acid in posteriorizing the neural ectoderm. Development, 2002. 129(18): p. 4335-46.